DALTON
FULL PAPER

Comparative DFT and X-ray structural studies of five-coordinate, N_4-donor macrocyclic ligand complexes of Cu(II) and Zn(II)

Leonard F. Lindoy,*[a] Torsten Rambusch,[a] Brian W. Skelton[b] and Allan H. White*[b]

[a] *Centre for Heavy Metals Research and School of Chemistry, The University of Sydney, N.S.W. 2006, Australia*
[b] *Department of Chemistry, The University of Western Australia, Nedlands, W.A. 6907, Australia*

Received 5th January 2001, Accepted 25th April 2001
First published as an Advance Article on the web 31st May 2001

A low-temperature single-crystal X-ray structural determination of $[CuCl(L^1)]ClO_4\cdot H_2O$ [where L^1 = *meso*-2,12-dimethyl-3,7,11,17-tetraazabicyclo[11.3.1]heptadeca-1(17),13,15-triene] is reported. The coordination geometry of the complex cation approximates square pyramidal, with the chloro ligand occupying an apical position. The latter group is associated with an intermolecular hydrogen bonding network involving the uncoordinated water molecule and the perchlorate counter ion. Density functional theory (DFT) has been applied to modeling the structure of this complex, both in the presence and the absence of the intermolecular hydrogen-bonding network. In the absence of this network a good fit to the X-ray structural parameters was obtained except for the Cu–Cl bond length. For this bond the calculated value (2.346 Å) was significantly shorter than the X-ray value [2.541(2) Å] but, on incorporation of the hydrogen-bonded network, while the major portion of the computed structure remained almost identical to that obtained from the initial calculation, the Cu–Cl bond was now found to be longer at 2.572 Å, approximating the X-ray value quite closely. The study has been extended to similar/related systems for which structural data are available, confirming the wider applicability of this approach in modeling arrays of this type.

Introduction

The evolution of computational chemistry, which has been facilitated by the development of ever more powerful CPU's in conjunction with more efficient calculational methods,[1] nowadays allows the calculation of large systems using fairly extended basis sets. In this context, density functional theory (DFT) has emerged as a computational method of choice for the solution of many chemical problems. This is because DFT methods have relatively low computational cost, include a significant amount of the dynamic electron correlation and are applicable to a wide range of molecular types, including transition metal complexes,[2] hydrogen bonded systems[3] and systems incorporating π interactions.[4] In addition, DFT methods are capable of giving results of quality comparable to those obtainable by correlated *ab initio* methods.

We now present the first report of the application of density functional theory in modelling a series of five co-ordinate complexes incorporating cations of the type $[MX(N_4\text{-macrocycle})]^+$ (where M = Cu or Zn, X = Cl or NCS). Specifically, the method has been employed to generate minimized structures for $[CuCl(L^1)]ClO_4\cdot H_2O$,[5] $[CuCl(L^4)]ClO_4\cdot H_2O$,[6] $[CuNCS(L^5)]^+$[7] and the structurally related zinc(II) complex, $[ZnCl(L^5)]^+$.[8] An aim of this study was to evaluate the use of DFT for modeling such five-coordinate species in the presence of two different types of electron configuration (d^9 and d^{10}), with emphases on probing the influence of intermolecular interactions (where present) on geometrical parameters which might be sensitive to these, in particular, the metal–apical halogen bond lengths.

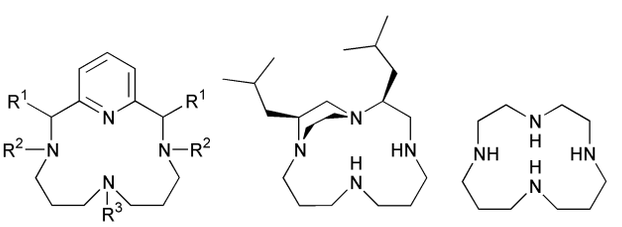

L^1 $R^1 = CH_3$, $R^2 = R^3 = H$
L^2 $R^1 = R^2 = R^3 = CH_3$
L^3 $R^1 = H$, $R^2 = R^3 = CH_3$
L^4
L^5

Experimental

Crystal structure determination of $[CuCl(L^1)]ClO_4\cdot H_2O$

Blue crystals of the above complex, grown from a diethyl ether–methanol mixture as described previously,[5] were found to be insufficiently substantial to support a single crystal structure determination with the sequential/single counter instrumentation then available. However, with the advent of a CCD/area-detector facility, the problem was revisited enabling the achievement of a definitive description of useful precision. A full sphere of data was measured at 153 K (Bruker AXS instrument; $2\theta_{max} = 58°$, ω scans; monochromatic Mo-Kα radiation, $\lambda = 0.7107_3$ Å), yielding 46890 independent reflections, merging to 5278 unique ($R_{int} = 0.095$) after 'empirical'/multiscan absorption correction, 2802 with $F > 4\sigma(F)$ considered 'observed' and used in the full matrix least squares refinement, refining anisotropic thermal parameter forms for the non-hydrogen atoms, and, also, $(x, y, z, U_{iso})_H$. Conventional residuals R, R_w (weights: $(\sigma^2(F) + 0.0004F^2)^{-1}$) at convergence were 0.067, 0.069. Pertinent results are given below and in Fig. 1 and Table 1.

Crystal data. $C_{15}H_{28}Cl_2CuN_4O_5$, $M = 478.9$. Orthorhombic, space group *Pbca* (D_{2h}^{15}, no. 61), $a = 16.816(3)$, $b = 12.065(4)$, $c = 20.293(4)$ Å, $V = 4117$ Å^3, D_c $(Z = 8) = 1.54_5$ g cm^{-3}, μMo = 13.5 cm^{-1}; specimen: $0.30 \times 0.15 \times 0.06$ mm; 'T'$_{min,max} = 0.56, 0.88$. $\Delta\rho_{max} = 1.15(6)$ e Å^{-3}.

DOI: 10.1039/b100250n

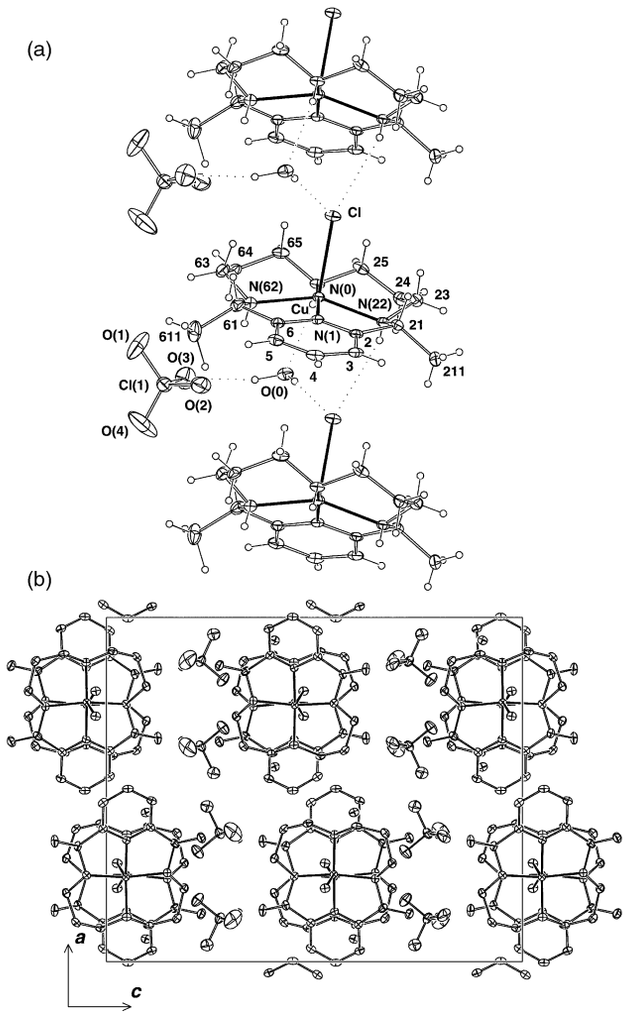

Fig. 1 (a) A hydrogen-bonded column of cations, anions and water molecules projected normal to its axis, *b*; 50% thermal ellipsoids are shown for the non-hydrogen atoms, hydrogen atoms having arbitrary radii of 0.1 Å. (b) Unit cell contents projected down the column axis, *b*, of the hydrogen-bonded arrays.

CCDC reference number 156018.

See http://www.rsc.org/suppdata/dt/b1/b100250n/ for crystallographic data in CIF or other electronic format.

Computational studies

All calculations were performed with the Amsterdam Density Functional 2000.02 (ADF)[9] program package on a Silicon Graphics Origin 2000 computer (56 MIPS R10000 64-Bit CPU with 195 MHz and 17 GB Memory). All structures were optimized without imposing symmetry constraints. The molecular orbitals were expanded in an uncontracted set of Slater-type orbitals (STOs) containing diffuse function. The basis is of double- or triple-zeta quality, augmented with one or two polarization functions. The cores were treated by the frozen-core approximation.[10] The numerical integration was performed using the procedure developed by Baerends *et al.*[11] The Becke–Perdew (BP86) functional was used for the calculations, using Becke's[12] gradient correction for the local expression of the exchange energy and Perdew's[13] gradient correction for the local expression of the correlation energy. The convergence criteria for the geometry optimizations, which use analytical derivatives,[14] were set to 1×10^{-3} hartree for the changes in energy, 1×10^{-3} hartree Å^{-1} for the energy gradient, 1×10^{-3} Å for the changes between old and new bond lengths, and 0.3° for changes in bond and dihedral angles. All stationary points on the hypersurface have been characterized as true minima by frequency analysis.

Table 1 Selected geometries (distances in Å, angles in °) for (a) [CuCl(L^1)]ClO$_4$·H$_2$O, with counterpart parameters for (b) [Cu(*N*CS)L^5]$^+$ (two molecules) and (c) [ZnClL^5]$^+$, five-coordinate complexes containing the pyridyl isocyclam derivative (L^1) and isocyclam (L^5)

Atoms	Parameters for (a); (b)(i),(ii); (c)
M–X	2.541(2); 2.292(6), 2.182(6); 2.2735(9)
M–N(1)	1.932(5); 2.025(5), 2.038(6); 2.200(3)
M–N(0)	1.994(6); 2.011(5), 2.010(5); 2.117(3)
M–N(22)	2.056(6); 2.041(5), 2.016(6); 2.084(3)
M–N(62)	2.041(6); 2.050(5), 2.024(6); 2.099(3)
X–M–N(1)	94.6(2); 89.1(2), 93.0(2); 98.85(8)
X–M–N(0)	94.7(2); 93.9(2), 94.4(2); 99.19(8)
X–M–N(22)	100.1(2); 100.6(2), 103.6(2); 108.41(9)
X–M–N(62)	102.8(2); 101.5(2), 100.3(2); 113.51(8)
N(1)–M–N(22)	81.3(2); 84.4(2), 83.8(2); 82.0(1)
N(1)–M–N(62)	81.9(2); 83.4(2), 82.8(2); 81.4(1)
N(0)–M–N(22)	97.6(3); 95.3(2), 94.5(2); 91.9(1)
N(0)–M–N(62)	95.5(3); 95.8(2), 95.7(2); 91.7(1)
N(1)–M–N(0)	170.7(2); 177.0(2), 172.6(2); 162.0(1)
N(22)–M–N(62)	152.5(3); 154.5(2), 153.1(2); 136.7(1)
	Out-of-(N$_4$)plane deviations δ/Å (negative toward X)
χ^2(N$_4$)	999; 2508, 1660; 11045
δN(1)	−0.107(7); −0.190(7), −0.160(7); −0.219(4)
δN(0)	−0.121(9); −0.156(7), −0.125(7); −0.190(4)
δN(22)	0.135(8); 0.173(7), 0.146(7); 0.204(4)
δN(62)	0.135(8); 0.173(7), 0.145(7); 0.205(4)
δM	−0.273(1); −0.226(1), −0.273(1); −0.542(1)
δC(2)	−0.01(1); 0.466(10), 0.49(1); 0.484(6)
δC(6)	−0.004(9); 0.394(9), 0.42(1); 0.490(5)
δC(21)	−0.22(1); −0.109(10), −0.04(1); −0.015(6)
δC(61)	−0.14(1); −0.162(10), −0.12(1); 0.000(6)
δC(23)	−0.40(1); −0.495(10), −0.50(1); −0.388(7)
δC(63)	−0.47(1); −0.435(11), −0.43(1); −0.396(6)
δC(24)	0.00(1); −0.108(1), −0.11(1); −0.063(7)
δC(64)	−0.15(1); −0.122(11), −0.10(1); −0.094(7)
δC(25)	−0.62(1); −0.754(10), −0.67(1); −0.729(7)
δC(65)	−0.75(1); −0.787(10), −0.70(1); −0.732(6)

The py(C$_5$N)/N$_4$ interplanar dihedral angle in [CuCl(L^1)]ClO$_4$·H$_2$O is 7.6(2)°. In [Cu(*N*CS)L^5]$^+$ amine hydrogen contacts are rather haphazard, one of the four sulfur atoms bridging is from each of the two cations, and two further sulfur atoms contact two hydrogens of the second cation; in summary, only one hydrogen of the first cation has a sulfur contact, while three of the second do, with three of the four sulfurs involved in such interactions. In [ZnClL^5]$^+$ three oxygens from the same perchlorate approach three of the hydrogens of the same cation, the fourth oxygen and hydrogen interacting as symmetry related species (see text).

Results and discussion

Crystal structure of [CuCl(L^1)]ClO$_4$·H$_2$O

Crystals of the above complex yielded a result consistent with the stoichiometry and connectivity represented by CuCl(ClO$_4$) : L^1 : H$_2$O (1 : 1 : 1). The aggregation of these moieties may more explicitly be described as [CuCl(L^1)]ClO$_4$·H$_2$O, as anticipated previously from physical measurements.[5] The ligand is associated with the metal atom, described to a first approximation as square-planar CuL^1, with a CuN$_4$ coordination sphere and the methyl substituents of the ligand are disposed quasi-equatorial, as is the pyridine ring (Fig. 1a). For the N$_4$ array χ^2 is 10^3, defining atom deviations δ N(0,1,22,62) being −0.121(9), −0.107(7), 0.135(8), 0.135(8) with δ Cu (non-defining) −0.273(1) Å. The angle sum about the copper atom is 356.$_3$°; the *trans* angles are more indicative of the departures from planarity of the environment, N(0)–Cu–(1) being 170.7(2) and N(22)–Cu–N(62) 152.5(3)°. While this distortion may be consistent with that expected to be consequent upon ring constraints (see below), it is also consistent with movement of the copper atom out of the macrocycle towards the chloride species which effectively occupies the apex of a square pyramidal array;

Cu–Cl is 2.541(2) Å, while Cu–Cu–N are all significantly above 90°. The Cu–N distances present as distinctly different: Cu–N(0,1) 1.994(6) and 1.932(5), with Cu–N(22,62), a pair at 2.056(6), 2.041(6) Å, the longest. While it is not unreasonable that Cu–N(1) be the shortest of the four by virtue of its incorporation as the central atom of the pair of smaller chelate rings (but the crowding here might be expected to have the converse effect of making it longer), rationalization of Cu–N(0) as shorter than Cu–N(22,62) is more clear cut because of the uncrowded approach of N(0), while the length of Cu–N(22,62) may in part reflect some Jahn–Teller effect.

The packing of the array (Fig. 1b) is of particular interest in the context of the present study (see later). The cations pack in columns within the unit cell, the Cu–Cl 'axis' broadly aligned with crystallographic *b*, and Cl contacting/hydrogen-bonding to the next (glide-related) cation: Cl ··· H(22) (N(22)) (½ − *x*, *y* − ½, *z*), 2.74(8) (3.301(6)) Å, as well as to a water molecule, the latter packing between cations at the periphery of the column (Cl ··· H(0b) (O(0)) (½ − *x*, *y* − ½, *z*) 2.45(7) (3.151(6)) Å), also contacted by one of the macrocycle amino hydrogens (H(0) (N(0)) ··· O 2.37(6) (3.030(9)) Å). The other hydrogen atom of the water molecule contacts the perchlorate anion (H(0a)(O(0)) ··· O(3) 2.10(8) (2.99(1)) Å), as does the other macrocycle amine hydrogen (H(62)(N(62)) ··· O(2) 2.47(6) (3.134(9)) Å) so that the perchlorate is also bound at the periphery of the column (Fig. 1a). The columns stack side by side thus forming a sheet about the *ab* face of the cell, the perchlorate ions forming a second sheet about $z = 0.25$ (Fig. 1b).

Aliphatic N_4-macrocycles such as of the parent '2,2,3,3' ('isocyclam'; 1,4,7,11-tetraazacyclotetradecane)[15] type coordinate in two basic modes about a central metal atom: quasi-planar in four-, five- or six-coordinate arrays such as in the present five-coordinate structure, and 'folded', as in a six-coordinate array where the planar disposition is precluded by occupancy of a pair of *cis* sites about the metal by a species such as ethane-1,2-diamine.[16] An example of the former type has been studied, to the extent of a force field calculation for the four-coordinate array $[NiL^5]^{2+}$ as its bis(perchlorate) salt (L^5 corresponds to L^1 minus the fused pyridine ring), the ring conformation having overall *m* symmetry.[17] This is closely paralleled by the disposition found in five-coordinate $[ZnClL^3]^{+}$[8] and $[Cu(NCS)L^3]^{+}$[7] (Table 1). The latter offer interesting comparisons in detail with the present structure; the six-membered rings in all cases have 'chair' conformations. Thus, the same overall conformation carries through to similar complexes of the present ligand, L^1, with the fused pyridine ring and adjacent equatorial methyl substituents, again in both four- {(β-)(red-)$[NiL^1][ClO_4]_2\cdot H_2O$},[18] five- $\{[CuClL^1]NO_3\cdot 2H_2O\}$[19] and, also, (*trans*-) six- $\{[Ni(NO_2)(ONO)L^1]\cdot ½\ H_2O\}$[20] coordinate arrays, the present five-coordinate array belonging here also. A different conformation is found in (yellow-)-(β-)$[NiL^1][ClO_4]_2$,[21] where one of the methyl substituents lies 'axial' with respect to the ring plane, the overall *m* symmetry being lost. Further variation may be imposed by the introduction of additional methyl substitution at the aliphatic nitrogen atoms of the present ligand to yield L^2, leading to the two forms described for $[NiXL^2][ClO_4]_n$, X = H_2O, $n = 2$; X = Cl, $n = 1$,[22] {the latter also found in $[CoClL^2]ClO_4$},[23] these in turn linking further afield to studies of complexes of 3,7,11-trimethyl-3,7,11,17-tetraazabicyclo[11.3.1]heptadeca-1(17),13,15-triene (L^3).[24]

Computational studies

A high-level DFT computational study of the structure of, and charge distribution within, $[Cu(L^1)Cl]ClO_4\cdot H_2O$ has been carried out in an attempt to model structural parameters found in the crystal structure of the above species which present a diversity of metal atom environments and ligand conformations in 'non-benign' lattices. For the present structure, the lowest observed minimum arrangement was highly symmetric (C_s), matching the square-pyramidal coordination geometry found in the X-ray study well. Fig. 2 shows the geometry of the calculated (BP86/TZPP) structure in the absence of intermolecular interactions. The calculated bond lengths (with the exception of the Cu–Cl length, see below) and angles display generally good agreement with the experimental values; comparison of the differences in the atom positions between the calculated and crystal structures gave an RMS value of 0.132 Å. A comparison of the respective copper-donor bond lengths is given in Table 2(a). While agreement between observed and calculated Cu–N bond lengths is fair, that for Cu–Cl was initially very poor. In this initial DFT calculation (for which intermolecular interactions were ignored) the Cu–Cl distance (2.346 Å) was calculated to be much shorter than that observed in the crystal structure (2.541(2) Å). The latter lies intermediate in the range (2.35–2.74 Å) observed for similar 'apical' Cu–Cl

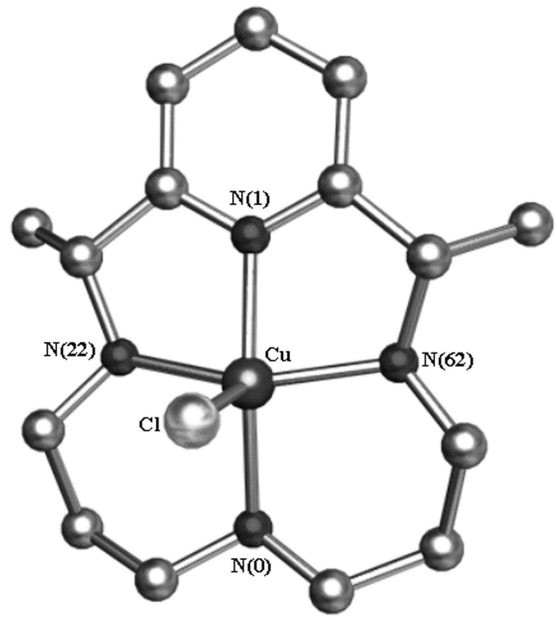

Fig. 2 DFT (BP86/TZPP) calculated minimum energy structure for $[CuCl(L^1)]^+$ in the absence of the hydrogen-bonding network.

Table 2 Comparison of the X-ray determined and calculated (BP86/TZPP) structures of $[CuClL^1]ClO_4\cdot H_2O$ (See Figs. 1–3)

(a) Copper–donor bond lengths/Å

Bond [a]	X-Ray	Calculated (BP86/TZPP)
Cu–Cl	2.541(2)	2.346 [b]
		2.572 [c]
Cu–N(0,1)	1.994(6), 1.932(5)	1.953, 1.917
Cu–N(22,62)	2.056(6), 2.041(6)	1.991, 1.991

(b) Hydrogen bond lengths (I–V)/Å in the intermolecular hydrogen-bonded network (See Fig. 3)

Bond	X-Ray	Calculated (BP86/DZP)
I [d]	2.10(8)	2.14
II [e]	2.47(7)	2.51
III [f]	2.37(6)	2.35
IV [g]	2.45(7)	2.39
V [h]	2.74(8)	2.71

[a] See Fig. 1 for numbering. [b] Intermolecular interactions not included. [c] Intermolecular interactions included (BP86/DZP). [d] Corresponding O(0) ··· O(3) length 2.99(1) (X-ray), 3.012 Å (calc.). [e] Corresponding N(62) ··· O(2) length 3.134(9) (X-ray), 3.142 Å (calc). [f] Corresponding N(0) ··· O(0) length 3.030(9) (X-ray), 3.051 Å (calc.). [g] Corresponding Cl ··· O(0) length 3.151(6) (X-ray), 3.170 Å (calc.). [h] Corresponding Cl ··· N(22) length 3.301(6) (X-ray), 3.275 Å (calc.).

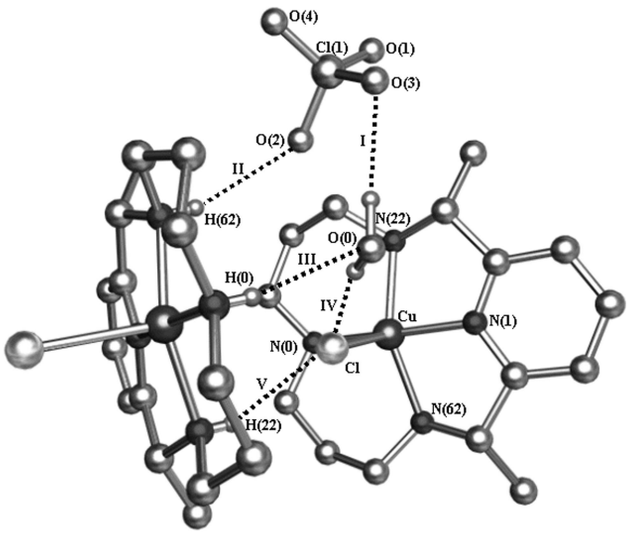

Fig. 3 The calculated (BP86/DZP) structure of $[CuCl(L^1)]ClO_4 \cdot H_2O$ incorporating the hydrogen-bonding environment (I–V) involving two copper complexes with one water molecule and one perchlorate anion.

bonds present in a series of related, square pyramidal copper(II) complexes[19,25] incorporating a planar N_4-donor macrocycle as reported in the Cambridge Crystallographic Database.[26]

As mentioned above, in this initial calculation the intermolecular hydrogen-bonding interactions observed in the X-ray determination were not considered. However, the calculation was then repeated with the above hydrogen bonding included, involving two complex cations linked through a water molecule, a perchlorate anion and a copper–bound chloride ligand in the manner shown in Fig. 3.

In this second calculation, as expected, the computed structure was almost identical to that obtained from the initial calculation, with the exception that the Cu–Cl bond was now much longer (2.572 Å), matching the experimental value [2.541(2) Å] quite closely. Fig. 3 shows the calculated (BP86/DZP) hydrogen-bonding environment of two complex molecules, with the hydrogen bonds represented by I–V; distances for the latter are compared in Table 2(b). The computed charge distribution within the hydrogen bonded array accords well with the presence of an intermolecular interaction between the chloride ion and the nearest macrocycle amine hydrogen H(22) of the neighbouring copper complex, corresponding to V, 2.71 Å. The water also exhibits a hydrogen bond to the chloride ion (IV; 2.39 Å), to one of the nearest nitrogen hydrogens of the neighbouring copper complex (III; 2.35 Å) and one to the oxygen O(3) of the perchlorate anion (I; 2.14 Å). A second oxygen atom, O(2), of the perchlorate anion contacts the macrocycle amine hydrogen (II; 2.51 Å) such that the perchlorate is also bound at the periphery of the array. A comparison of internuclear distances for the heavy atoms associated with hydrogen bonds I–V is given in a footnote to Table 2(b); the experimentally determined values and the DFT calculated ones are in good agreement, with differences lying between 0.008 and 0.026 Å.

Calculations on a second five-coordinate copper(II) complex of type $[CuClL^4]ClO_4 \cdot H_2O$, whose coordinates were taken[27] from the Cambridge Crystallographic Database, also resulted in a good reproduction of the structure of the solid complex using the DFT functional BP86. Once again, an intermolecular hydrogen bonding network is associated with the 'apical' chloro ligand in this complex. As in the previous study, the calculated Cu–Cl distance (2.33 Å) in the absence of the intermolecular interactions was found to be significantly shorter than that observed in the crystal structure [2.478(3) Å], but, again, the other geometrical details were in very good agreement with the X-ray structural data [Table 3(a)]. On modeling the structure with the intermolecular interactions included, a clear elongation of the Cu–Cl bond (to 2.49 Å) occurred, matching the experimental value quite closely. The calculated (BP86/DZP) hydrogen-bonding environment, composed of two complex cations together with an associated water molecule and perchlorate anion, is shown in Fig. 4. The hydrogen bonds are represented by I–V [see Table 3(b)]. The computed charge distribution within the hydrogen bonded array accords well with the presence of a significant intermolecular interaction between the chloride ion and the nearby water hydrogen (V; 2.36 Å).

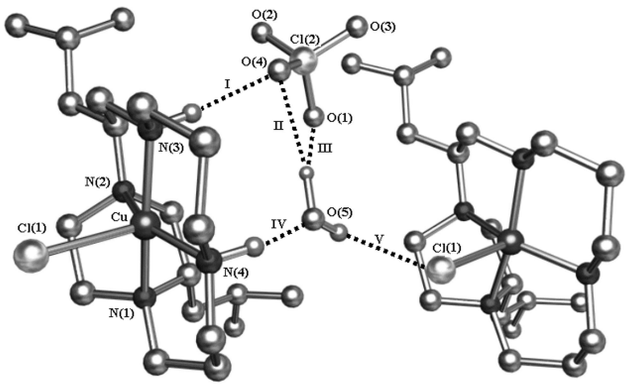

Fig. 4 The calculated (BP86/DZP) structure of $[CuClL^4]ClO_4 \cdot H_2O$ incorporating the hydrogen-bonding environment (I–V) involving two copper complexes with one water molecule and one perchlorate anion (CCDC numbering).

Table 3 Comparison of the X-ray determined and calculated (BP86/DZP) structures of $[CuClL^4]ClO_4 \cdot H_2O$ (See Fig. 4)

(a) Copper–donor bond lengths/Å

Bond	X-Ray	Calculated
Cu–Cl	2.478(3)	2.490 [a]
		2.334 [b]
Cu–N(1)	2.040(11)	2.052
Cu–N(2)	2.045(11)	2.053
Cu–N(3)	1.998(7)	2.002
Cu–N(4)	2.006(10)	2.004

(b) Hydrogen bond lengths (I–V) Å in the intermolecular hydrogen-bonded network

Bond	X-Ray	Calculated
I	2.09	2.11
II	2.27	2.17
III	2.16	2.17
IV	1.98	2.00
V	2.39	2.36

[a] Intermolecular interactions included. [b] Intermolecular interactions not included.

The other water molecule hydrogen contacts two oxygens of the perchlorate anion (II, III; both 2.17 Å) with the oxygen contacting one of the nearest nitrogen hydrogen of the neighbouring copper complex (IV; 2.00 Å). A further oxygen atom, of the perchlorate anion, contacts another amine hydrogen (I; 2.11 Å).

The above results for the cationic copper chloride derivatives of L^1 and L^4 clearly demonstrate that inclusion of the associated intermolecular interactions present in the respective solid-state geometries is necessary for good reproduction of the apical Cu–Cl bond lengths in such complexes.

In order to probe the wider applicability of the computational procedures discussed above, a further two structurally related (five-coordinate) complexes of 1,4,7,11-tetraazacyclotetradecane (isocyclam), L^5, incorporating copper(II) and zinc(II), were investigated. These derivatives contain the com-

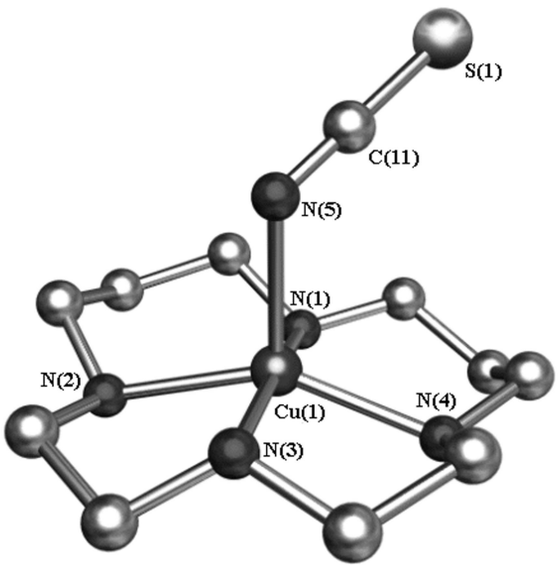

Fig. 5 The calculated geometry (BP86/TZPP) of the lowest found minimum structure of $[Cu(NCS)L^5]^+$ (Cation 1).

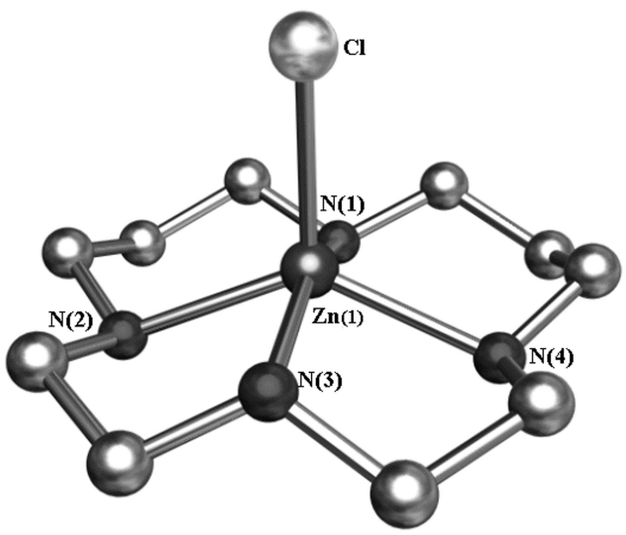

Fig. 6 The calculated geometry (BP86/TZPP) of the lowest found minimum structure of $[ZnClL^5]^+$.

plex cations, $[Cu(NCS)L^5]^+$ [7] and $[ZnClL^5]^+$, respectively.[8] X-Ray data for the latter complexes were taken from the Cambridge Crystallographic Database. These complexes differ from those discussed above in that no hydrogen-bonding network involving the 'apical' isothiocyanato or chloro ligands is present in the solid state.

The calculated [BP86/TZPP] structures of the copper and zinc complexes are shown in Figs. 5 and 6, while Tables 4 and 5 provide a comparison of selected bond lengths obtained from the corresponding crystal and the calculated structures. Once again, very good agreement occurs between both sets of data, further substantiating the applicability of the DFT method BP86 for the calculation of complexes of the present type.

Conclusion

The DFT calculations have been quite successful in modelling the structures of $[CuCl(L^1)]ClO_4 \cdot H_2O$, $[CuClL^4]ClO_4 \cdot H_2O$, $[Cu(NCS)L^5]^+$ and $[ZnClL^5]^+$. In particular, it has been demonstrated that the inclusion of observed intermolecular interactions in the model for the first two of these complexes is necessary for good reproduction of the Cu–Cl bond lengths observed in the solid complexes. Conversely, the calculations clearly demonstrate the influence that hydrogen bonding can have on apical ligand bond lengths in such square pyramidal copper(II) complexes. The results also serve to illustrate the excellent performance of the DFT gradient corrected Becke–Perdew functional BP86 in the ADF package for modeling systems of the present type.

Table 4 Comparison of selected bond lengths (Å) in the crystal structure and calculated (BP86/TZPP) structure of $[Cu(NCS)L^5]^+$

Bond [a]	X-Ray	Calculated
Cu–N(1,6)	2.041(5), 2.016(6)	2.022
Cu–N(2,7)	2.011(5), 2.010(5)	2.019
Cu–N(3,8)	2.050(5), 2.024(6)	2.044
Cu–N(4,9)	2.025(5), 2.038(6)	2.048
Cu–N(5,10)	2.292(6), 2.182(6)	2.191

[a] CCDC numbering.

Table 5 Comparison of selected bond lengths (Å) in the crystal structure and calculated (BP86/TZPP) structure of $[ZnClL^5]^+$

Bond [a]	X-Ray	Calculated
Zn–Cl	2.273(9)	2.258
Zn–N(1)	2.117(3)	2.109
Zn–N(2)	2.084(3)	2.101
Zn–N(3)	2.200(3)	2.203
Zn–N(4)	2.099(3)	2.106

[a] CCDC and ref. 8 numbering.

Acknowledgements

We thank the Australian Research Council for assistance. T. R. also thanks the Deutscher Akademischer Austauschdienst (DAAD) for support.

References

1 K. R. Adam and L. F. Lindoy, in *Crown Compounds: Towards Future Applications*, ed. S. R. Cooper, VCH, Weinheim, 1992, pp. 69–79; *DFT Methods in Chemistry and Material Science*, ed. M. Springborg, Wiley, New York, 1997; *Electronic Density Functional Theory: Recent Progress and New Directions*, eds. J. Dobson, G. Vignale and M. P. Das, Plenum, New York, 1998; H. Chermette, *Coord. Chem. Rev.*, 1998, **178–180**, 699.
2 See, for example: K. R. Adam, I. M. Atkinson and L. F. Lindoy, *Inorg. Chem.*, 1997, **36**, 480; S. Kirsch, B. Noll, H. Spies, P. Leibnitz, D. Scheller, T. Krueger and B. Johannsen, *J. Chem. Soc., Dalton Trans.*, 1998, 455; T. Rambusch, K. Hollmann-Gloe and K. Gloe, *J. Prakt. Chem.*, 1999, **341**, 202.
3 See, for example: J. Fabian, K. Gloe, M. Wuest, T. Krueger-Rambusch, O. Rademacher and H. Graubaum, *Phosphorus, Sulfur Silicon Relat. Elem.*, 1998, **140**, 35; C. F. Guerra, F. M. Bickelhaupt, J. G. Snijders and E. J. Baerends, *J. Am. Chem. Soc.*, 2000, **122**, 4117.
4 See, for example: L. Scaccianoce, D. Braga, M. J. Calhorda, F. Grepioni and B. F. G. Johnson, *Organometallics*, 2000, **19**, 790; M. Oki, S. Takano and S. Toyota, *Bull. Chem. Soc. Jpn.*, 2000, **73**, 2221.
5 L. F. Lindoy, N. E. Tokel, L. B. Anderson and D. H. Busch, *J. Coord. Chem.*, 1971, **1**, 7.
6 Y. Kojima, Y. Seki, S. Yasuda, K. Hirotsu and H. Miyake, *Acta Crystallogr., Sect. C*, 1998, **54**, 1602.
7 T. H. Tahirov, T.-H. Lu, W. J. Lan and C.-S. Chung, *Acta Crystallogr., Sect. C*, 1993, **49**, 1908.
8 T.-H. Lu, K. Panneerselvam, S.-F. Tung, T.-Y. Chi and C.-S. Chung, *Acta Crystallogr., Sect. C*, 1997, **53**, 1780.
9 ADF Version 2000.02, Scientific Computing & Modelling, Vrije Universiteit, Amsterdam; G. te Velde and E. J. Baerends, *J. Comput. Phys.*, 1992, **99**, 84; C. F. Guerra, J. G. Snijders, G. te Velde and E. J. Baerends, *Theor. Chem. Acc.*, 1998, **99**, 391.
10 E. J. Baerends, D. E. Ellis and P. Ros, *Chem. Phys.*, 1973, **2**, 41.
11 P. Boerrigter, G. te Velde and E. J. Baerends, *Int. J. Quantum Chem.*, 1988, **33**, 87; G. te Velde and E. J. Baerends, *Int. J. Quantum Chem.*, 1992, **37**, 84.
12 A. D. Becke, *Phys. Rev. A*, 1988, **38**, 3089.

13 J. P. Perdew, *Phys. Rev. B*, 1986, **33**, 8822; J. P. Perdew, *Phys. Rev. B*, 1986, **34**, 7406.
14 L. Versluis and T. Ziegler, *J. Chem. Phys.*, 1988, **88**, 322.
15 A. Dei, L. Fabbrizzi and P. Paoletti, *Inorg. Chem.*, 1981, **20**, 4035.
16 L. F. Lindoy, *The Chemistry of Macrocyclic Ligand Complexes*, Cambridge University Press, Cambridge, 1989.
17 J. C. A. Boeyens, *Acta Crystallogr., Sect. C*, 1983, **39**, 846.
18 M. G. B. Drew and S. Hollis, *Acta Crystallogr., Sect. B*, 1980, **36**, 718.
19 M. R. Caira, L. R. Nassimbeni and P. R. Woolley, *Acta Crystallogr., Sect. B*, 1975, **31**, 1334.
20 M. G. B. Drew and S. Hollis, *Acta Crystallogr., Sect. B*, 1980, **36**, 1944.
21 R. Dewar and E. Fleischer, *Nature (London)*, 1969, **222**, 372.
22 C.-M. Che, S.-T. Mak, W.-O. Lee, K.-W. Fong and T. C. W. Mak, *J. Chem. Soc., Dalton Trans.*, 1988, 2153.
23 C.-M. Che, S.-T. Mak and T. C. W. Mak, *Inorg. Chem.*, 1986, **25**, 4705.
24 K. A. Foster, E. K. Barefield and D. G. V. Derveer, *J. Chem. Soc., Chem. Commum.*, 1986, 680; N. A. Alcock, P. Moore and H. A. A. Omar, *J. Chem. Soc., Dalton Trans.*, 1987, 1107.
25 T. Sakurai, K. Kobayashi, A. Hasegawa, S. Tsuboyama and K. Tsuboyama, *Acta Crystallogr., Sect. B*, 1982, **38**, 107; K. Kobayashi, T. Sakurai, A. Hasegawa, S. Tsuboyama and K. Tsuboyama, *Acta Crystallogr., Sect. B*, 1982, **38**, 1154; T. Sakurai, K. Kobayashi, H. Masuda, S. Tsuboyama and K. Tsuboyama, *Acta Crystallogr., Sect. C*, 1983, **39**, 334; J. M. Harrowfield, A. M. Sargeson, B. W. Skelton and A. H. White, *Aust. J. Chem.*, 1994, **47**, 181; R. J. Lancashire, P. D. Newman, F. S. Stephens, R. S. Vagg and P. A. Williams, *J. Coord. Chem.*, 1995, **34**, 339; M. R. Sundberg, R. Sillanpaa and R. Uggla, *Inorg. Chim. Acta*, 1996, **245**, 35; P. V. Bernhardt and P. C. Sharpe, *Chem. Commun.*, 1996, 1267; P. V. Bernhardt, J. C. Hetherington and L. A. Jones, *J. Chem. Soc., Dalton Trans.*, 1996, 4325.
26 Cambridge Crystallographic Database Version 5.15, CCDC, Cambridge, 2000.
27 Y. Kojima, Y. Seki, S. Yasuda, K. Hirotsu and H. Miyake, *Acta Crystallogr., Sect. C*, 1998, **54**, 1602.